

Wave Propagation and Mode Localization in Simply Supported Multispan Beams with Couplers on Supports

By Dong Ok Kim*, Byoung Wan Kim**, Jong-Heon Lee*** and In Won Lee****

Abstract

This paper studies the influences of coupler on wave propagation and mode localization in simply supported multispan beams with couplers consisting of lumped rotational stiffness and mass on supports. A transfer matrix governing vibrational wave propagation in simply supported multispan beams with couplers is newly derived and simplified. The eigenvalue of the simplified transfer matrix shows that the larger stiffness or the larger mass of the coupler weakens internal coupling between spans, thereby making the system more sensitive to mode localization. Mass effect increases while stiffness effect decreases with increasing wave frequency or eigenvalue of the system. A region with relatively wider passbands and narrower stopbands with small attenuation rates is noted when large stiffness and mass are considered at the same time. The regions normal modes are also delocalized. As an example structure, simply supported two-span beam with a coupler at the midspan is considered.

Keywords: wave propagation, mode localization, couplers

1. Introduction

Many engineering structures are made of identical sub-structures connected by couplers, shaping into periodic structures. For some periodic structures, the presence of small irregularities breaking the assumption of structural identity may significantly affect mode shapes of the structures and may be a cause of mode localization. Mode localization results in that the vibration energy of the mode is confined to specific regions and so the structure may suffer unpredicted local damages and the performance of a motion controller of the structure might decrease abruptly.

In solid-state physics, the localization phenomenon of electron field in disordered solid was first observed by Anderson (1958) who shared the 1977 Nobel Prize in physics for his work. Hodges (1982) was the first to recognize that the wave localization may occur in the disordered periodic structures and it leads to mode localization. In many works (Bendiksen, 1987 ; Bouzit and Pierre, 1992 ; Cornwell and Bendiksen, 1987 ; Cornwell and Bendiksen, 1989 ; Langley, 1995 ; Lust *et al.*, 1993 ; Pierre and Dowell, 1987

; Pierre *et al.*, 1987), various structures have been considered and many methods have been proposed to discuss the characteristics of mode localization.

It is well known that, under a condition of weak coupling by couplers stiffness, the mode shapes undergo dramatic changes to become strongly localized when small disorder is introduced. To date, however, little attention has been paid to the influences of the mass of coupler on coupling strength and mode localization.

The present study is an attempt to prove that the mass, as well as the stiffness, of the coupler exerts important influences upon mode localization and weak coupling conditions. This work is an extended work of Kim and Lee (1999) in which a simple lumped system was considered. In the second section of this paper, a transfer matrix equation governing the vibrational wave propagation in the simply supported multispan beams with couplers is derived and simplified for theoretical study. In the next section, using the eigenvalue of the simplified transfer matrix, the influences of the coupler consisting of a lumped rotational stiffness and a lumped rotational mass on coupling strength and

*Senior Researcher, Mechanical Systems Development Department, KAERI, Korea (E-mail: dokim@kaeri.re.kr)

**Graduate Student, Department of Civil and Environmental Engineering, KAIST, Korea (E-mail: kimbw@kaist.ac.kr)

***Member, Professor, Department of Civil Engineering, Kyungil University, Korea (E-mail: honey55@hosanna.net)

****Member, Professor, Department of Civil and Environmental Engineering, KAIST, Korea (E-mail: iwlee@kaist.ac.kr)

on wave propagation are discussed. Section four is an example verifying the influences of coupler on mode localization, where a simply supported two span beam with a coupler at the mid-support is considered.

2. Formulations

In this section a transfer matrix equation governing the wave propagation in simply supported multispan beams with couplers on supports is formulated. Fig. 1 shows the structure considered. Each span has the flexural rigidity EI , the mass density m and the length $2L_j$. The j -th coupler consists of a lumped rotational stiffness K_j and a lumped rotational mass J_j . The coordinate system of the j -th span is shown in Fig. 2. An eigenvalue problem representing the free vibration of j -th span is as follows:

$$\frac{d^4 y_j(x_j)}{dx_j^4} - \lambda^4 y_j(x_j) = 0 \tag{1}$$

where λ is eigenvalue of the system having natural frequency ω_n and has the following relationship.

$$\lambda^2 = \omega_n^2 \frac{m}{EI} \tag{2}$$

General solution of Eq. (1) may be assumed as

$$y_j(x_j) = A_j \cosh \lambda x_j + B_j \sinh \lambda x_j + C_j \cos \lambda x_j + D_j \sin \lambda x_j \tag{3}$$

where the constants A_j , B_j , C_j and D_j may be determined by applying boundary conditions of the j -th span. By applying the simple support conditions of each span, such as $y_j(L_j) = 0$ and $y_j(L_j) = 0$. Eq. (3) is reduced to

$$y_j(x_j) = C_j \left(\cos \lambda x_j - \frac{\cos \lambda L_j}{\cosh \lambda L_j} \cosh \lambda x_j \right) + D_j \left(\sin \lambda x_j - \frac{\sin \lambda L_j}{\sinh \lambda L_j} \sinh \lambda x_j \right) \tag{4}$$

Applications of the slope and moment continuity conditions for any consecutive spans j and $j + 1$ on Eq. (4) and



Fig. 1. Simply Supported Continuous N-span Beam with Couplers at Supports

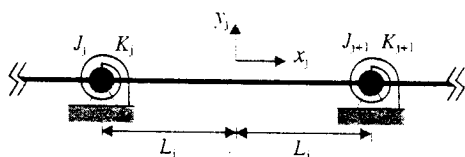


Fig. 2. Coordinate System of the j -th Span

simplification yield a single matrix equation as follows:

$$T_{j-1} y_j = y_{j-1} \tag{5}$$

where

$$y_j = \begin{Bmatrix} C_j \\ D_j \end{Bmatrix} \text{ and } y_{j+1} = \begin{Bmatrix} C_{j+1} \\ D_{j+1} \end{Bmatrix} \tag{6}$$

$$T_{j-1} = \left(1 - \frac{\sin 2\lambda L_{j+1}}{\sin 2\lambda L_{j-1}} \right)^{-1} \begin{bmatrix} T_{11} & T_{12} \\ T_{21} & T_{22} \end{bmatrix} \tag{7}$$

$$T_{11} = \psi_{j-1} \cos \lambda L_j - \theta_j \sin \lambda L_{j-1} + \frac{K_{j-1} - \omega_n^2 J_{j-1}}{2\lambda EI} \theta_j \psi_{j-1} \tag{8a}$$

$$T_{12} = \psi_{j-1} \sin \lambda L_j - \psi_j \sin \lambda L_{j-1} + \frac{K_{j-1} - \omega_n^2 J_{j-1}}{2\lambda EI} \psi_j \psi_{j-1} \tag{8b}$$

$$T_{21} = -\theta_{j-1} \cos \lambda L_j - \theta_j \cos \lambda L_{j-1} + \frac{K_{j-1} - \omega_n^2 J_{j-1}}{2\lambda EI} \theta_j \theta_{j-1} \tag{8c}$$

$$T_{22} = -\theta_{j-1} \sin \lambda L_j - \psi_j \cos \lambda L_{j-1} + \frac{K_{j-1} - \omega_n^2 J_{j-1}}{2\lambda EI} \psi_j \theta_{j-1} \tag{8d}$$

and

$$\theta = -\sin \lambda L + \tanh \lambda L \cos \lambda L, \text{ and } \psi = \cos \lambda L - \coth \lambda L \sin \lambda L. \tag{9}$$

Eq. (5) is a transfer matrix equation associated with the propagation of vibration between adjacent two spans. Applications of the moment equilibrium conditions defined at the both ends of the structure on Eq. (4) yield the two boundary conditions as follows:

$$b_{1j}^T y_j = 0 \text{ and } b_{n-1}^T y_n = 0 \tag{10}$$

where the boundary condition vectors are

$$b_j = \begin{Bmatrix} -\cos \lambda L_j - \frac{K_j - \omega_n^2 J_j}{2\lambda EI} \theta_j \\ -\sin \lambda L_j - \frac{K_j - \omega_n^2 J_j}{2\lambda EI} \psi_j \end{Bmatrix} \text{ and } b_{n+1} = \begin{Bmatrix} -\cos \lambda L_n - \frac{K_{n+1} - \omega_n^2 J_{n+1}}{2\lambda EI} \theta_n \\ -\sin \lambda L_n - \frac{K_{n+1} - \omega_n^2 J_{n+1}}{2\lambda EI} \psi_n \end{Bmatrix} \tag{11}$$

Combining the transfer matrix equation, Eq. (5) and the boundary conditions, Eq. (10), gives the characteristic equation of the system as follows.

$$f(\lambda) = \beta_{n+1}^T \left[\prod_{k=1}^n T_{k-1} \right] \begin{bmatrix} 0 & -1 \\ 1 & 0 \end{bmatrix} b_1 = 0 \tag{12}$$

By solving the characteristic equation, we get the eigenvalues of the system. Repeated application of Eq. (5) start-

ing with an assumption of $y_1 = [0, -1; 1, 0]b_1$ and the eigenvalue given by solving Eq. (12) yields all the state vectors y_j 's of the spans and finally we get the eigenvectors of the system.

Numerical study using the transfer matrix equation, the boundary conditions and the characteristic equation may give many interesting results. However, since there are hyperbolic terms, it is almost impossible to study theoretically with those equations and conditions. Therefore it is desirable to make them simple for the theoretical study. Fortunately, since the terms of hyperbolic tangent and hyperbolic cotangent in the equations converge to unity very quickly with the increase of λL_j and λL_{j+1} , under the assumptions of $\lambda L_j > 1$ and $\lambda L_{j+1} > 1$ the transfer matrix can be simplified as

$$T_{j+1} = R(-\lambda L_{j+1})C(c_{j+1})R(-\lambda L_j) \quad (13)$$

where $R(-\lambda L_{j+1})$ and $R(-\lambda L_j)$ are rotation matrices written as:

$$R(-\lambda L_{j+1}) = \begin{bmatrix} \cos \lambda L_{j+1} & \sin \lambda L_{j+1} \\ -\sin \lambda L_{j+1} & \cos \lambda L_{j+1} \end{bmatrix} \text{ and}$$

$$R(-\lambda L_j) = \begin{bmatrix} \cos \lambda L_j & \sin \lambda L_j \\ -\sin \lambda L_j & \cos \lambda L_j \end{bmatrix} \text{ and} \quad (14)$$

$C(c_{j+1})$ has the following form

$$C(c_{j+1}) = c_{j+1} \begin{bmatrix} 1 & 1 \\ -1 & 1 \end{bmatrix} + \begin{bmatrix} 0 & 1 \\ -1 & 0 \end{bmatrix} \quad (15)$$

where

$$c_{j+1} = 1 + \frac{1}{\lambda L} [\bar{K}_{j+1} - \bar{J}_{j+1} (\lambda L)^2] \quad (16)$$

As you can see, c_{j+1} is a function of λL and the stiffness and mass of the coupler, where L is an arbitrary reference half-span length and \bar{K}_{j+1} and \bar{J}_{j+1} are dimensionless stiffness and mass

$$\bar{K}_{j+1} = \frac{1}{2} \frac{K_{j+1} L}{EI} \text{ and } \bar{J}_{j+1} = \frac{1}{2} \frac{J_{j+1}}{mL^3} \quad (17)$$

Under the same assumptions of $\lambda L_1 > 1$ and $\lambda L_n > 1$, the boundary condition vectors in Eq. (11) may be simplified as

$$b_1 = -R(-\lambda L_1) \begin{Bmatrix} c_1 \\ c_1 - 1 \end{Bmatrix} \text{ and}$$

$$b_{n+1} = R(\lambda L_n) \begin{Bmatrix} -c_{n+1} \\ c_{n+1} - 1 \end{Bmatrix} \quad (18)$$

3. Wave Propagation

The behavior of energy-carrying waves can be characterized by the eigenvalues of the transfer matrix. In this study, the transfer matrix has two eigenvalues given by solving

$$\det[T_{j+1} - \lambda_w I] = 0 \quad (19)$$

where λ_w is an eigenvalue of the transfer matrix and I is a 2×2 identity matrix. Considering the case of $L_{j+1} = L_j$, it is easy to show that the eigenvalues have the form of $\lambda_w = e^{\pm \mu}$ where μ is wave propagation constant. Generally the wave propagation constant is a complex number, such as $\mu = \gamma + j\sigma$. The real part of the propagation constant, γ , is the rate of exponential attenuation of the wave amplitude and the imaginary part, σ , is the difference in phase between the motion of adjacent spans. Fig. 3 shows γ and σ of the case of $L_{j+1} = L_j = L$ and $\bar{K}_{j+1} = \bar{J}_{j+1} = 0$ ($c_{j+1} = 1$) as functions of $\lambda L / \pi$. The regions of $\gamma = 0$ are passbands and the regions of $\gamma \neq 0$ are stopbands. The waves in passbands propagate without attenuation in magnitude. In the stopbands only attenuated standing waves can exist. In what follows, the influences of the stiffness and mass of a coupler on the passband/stopband structure are studied.

Using the simplified transfer matrix with $L = (L_{j+1} + L_j) / 2$ leads the eigenvalues to

$$\lambda_w = \sqrt{c_{j+1}^2 + 1} \cos(2\lambda L + \phi_{j+1}) \pm \sqrt{(c_{j+1}^2 + 1) \cos^2(2\lambda L + \phi_{j+1}) - 1} \quad (20)$$

where

$$\phi_{j+1} = \tan^{-1} \frac{1}{c_{j+1}} \quad (21)$$

Since the passband is a region where the propagation constant has no real part, from Eq. (20) one can conclude that the regions of λL satisfying following conditions are passbands: when $c_{j+1} < 0$ or $\phi_{j+1} > 0$,

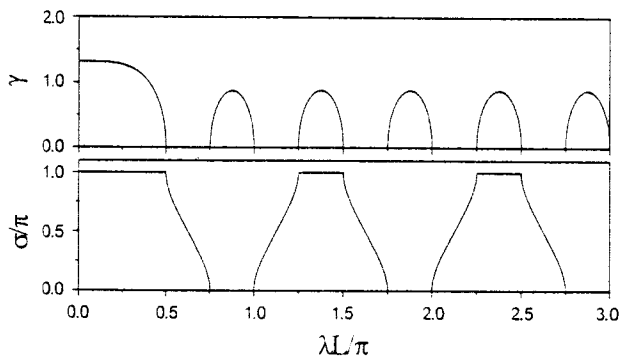


Fig. 3. Wave Propagation Constant of a Transfer Matrix with Identical Span Lengths in Adjacent Two Spans and without Coupler

$$\frac{2n+1}{4}\pi - \phi_{j+1} \leq \lambda L \leq \frac{2n+1}{4}\pi, n = 1, 2, \dots \quad (22)$$

and where $c_{j+1} < 0$ or $\phi_{j+1} < 0$.

$$\frac{2n+1}{4}\pi \leq \lambda L \leq \frac{2n+1}{4}\pi - \phi_{j+1}, n = 1, 2, \dots \quad (23)$$

Considering the case of $c_{j+1} = 1$ or $\phi_{j+1} = \pi/4$ ($\bar{K}_{j+1} = \bar{J}_{j+1} = 0$) when $\lambda L > 1$, the passbands represented by the above first condition are consistent with those in Fig. 3. The width of a passband will be increased with the decrease of c_{j+1} or the increase of ϕ_{j+1} . Another remarkable interesting result is that a certain λL causing $c_{j+1} = 0$ or $\phi_{j+1} = \pm\pi/2$ is always in a passband.

It is well known that the large \bar{K}_{j-1} is the cause of weak internal coupling and a pre-occurrence of the drastic occurrence of mode localization. Generally, the coupling strength

is measured by $1/\bar{K}_{j+1}$ but it is not suited to the cases of considering \bar{K}_{j+1} and \bar{J}_{j+1} at the same time. In this paper, the angel is proposed as a measure of coupling strength C_S . If all the couplers in a multispan beam have the identical properties, one can rewrite ϕ_{j+1} without the subscript and the coupling strength representing the strengths of internal couplings between spans of the structure can be defined as

$$C_S \equiv \phi \quad (24)$$

Mature consideration with Eqs (16) and (21) and the two conditions defined by Eqs (22) and (23) may yield interesting results. The larger stiffness of coupler results in smaller C_S in the lower frequency range and the larger mass of coupler results in smaller C_S in the higher frequency range. Fig. 4 shows the influences of \bar{K}_{j+1} and \bar{J}_{j+1} on the pass-

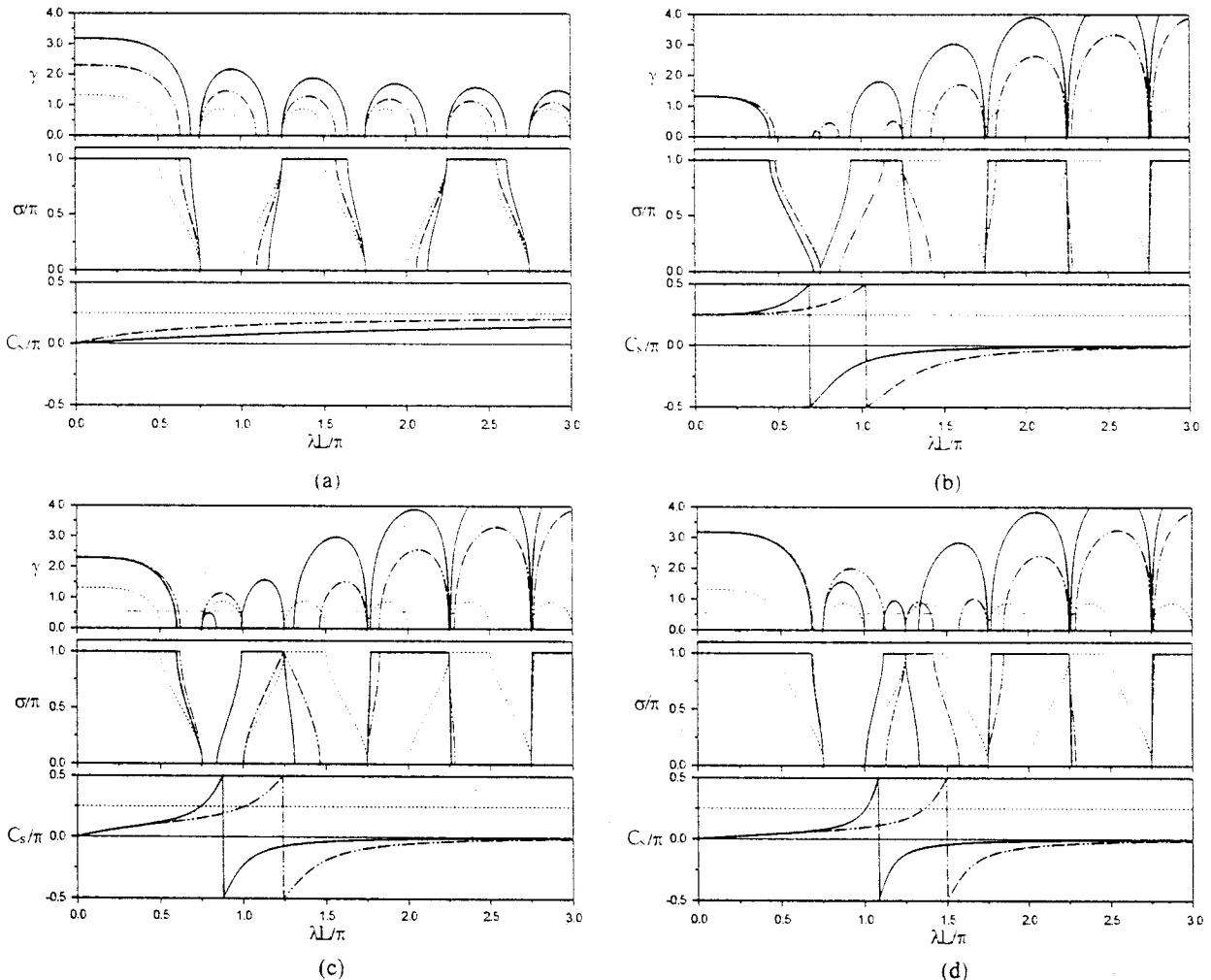


Fig. 4. Influences of a Coupler on the Passband/Stopband Structure. Where γ is Real Part of Propagation Constant and σ Imaginary Part.

The dotted lines (.....) represent the case of $\bar{K} = 0.0, \bar{J} = 0.0$; (a) ---: $\bar{K} = 3.0, \bar{J} = 0.0$; —: $\bar{K} = 10.0, \bar{J} = 0.0$; (b) ---: $\bar{K} = 0.0, \bar{J} = 0.03$; —: $\bar{K} = 0.0, \bar{J} = 0.1$; (c) ---: $\bar{K} = 3.0, \bar{J} = 0.0$; —: $\bar{K} = 3.0, \bar{J} = 0.1$; (d) ---: $\bar{K} = 10.0, \bar{J} = 0.03$; —: $\bar{K} = 10.0, \bar{J} = 0.1$

band/stopband structures and the variations of coupling strength C_S as functions of $\lambda L/\pi$. As predicted, the larger \bar{K}_{j+1} or \bar{J}_{j+1} leads to smaller C_S causing narrower passbands and wider stopbands with larger rate of exponential attenuation. The influence of the mass increases with the increase of λL while the influence of the stiffness decreases. A certain λL leading to $C_S = \pm\pi/2$ (or $c_{j+1} = 0$) is always in a passband.

Since mode localization occurs when a mode on the edge of a passband is moved to the stopband by disordering the periodic structure, the weak internal coupling causing narrow passbands and large attenuation rates is precondition of



Fig. 5. Simply Supported Two-Span Beam with a Coupler at the Midsupport

drastic occurrence of mode localization. Therefore, the larger stiffness of coupler may increase the sensitivity to mode localization of the modes in lower frequency range and the larger mass may do in higher frequency range. In the next section, these influences will be verified with a simple example.

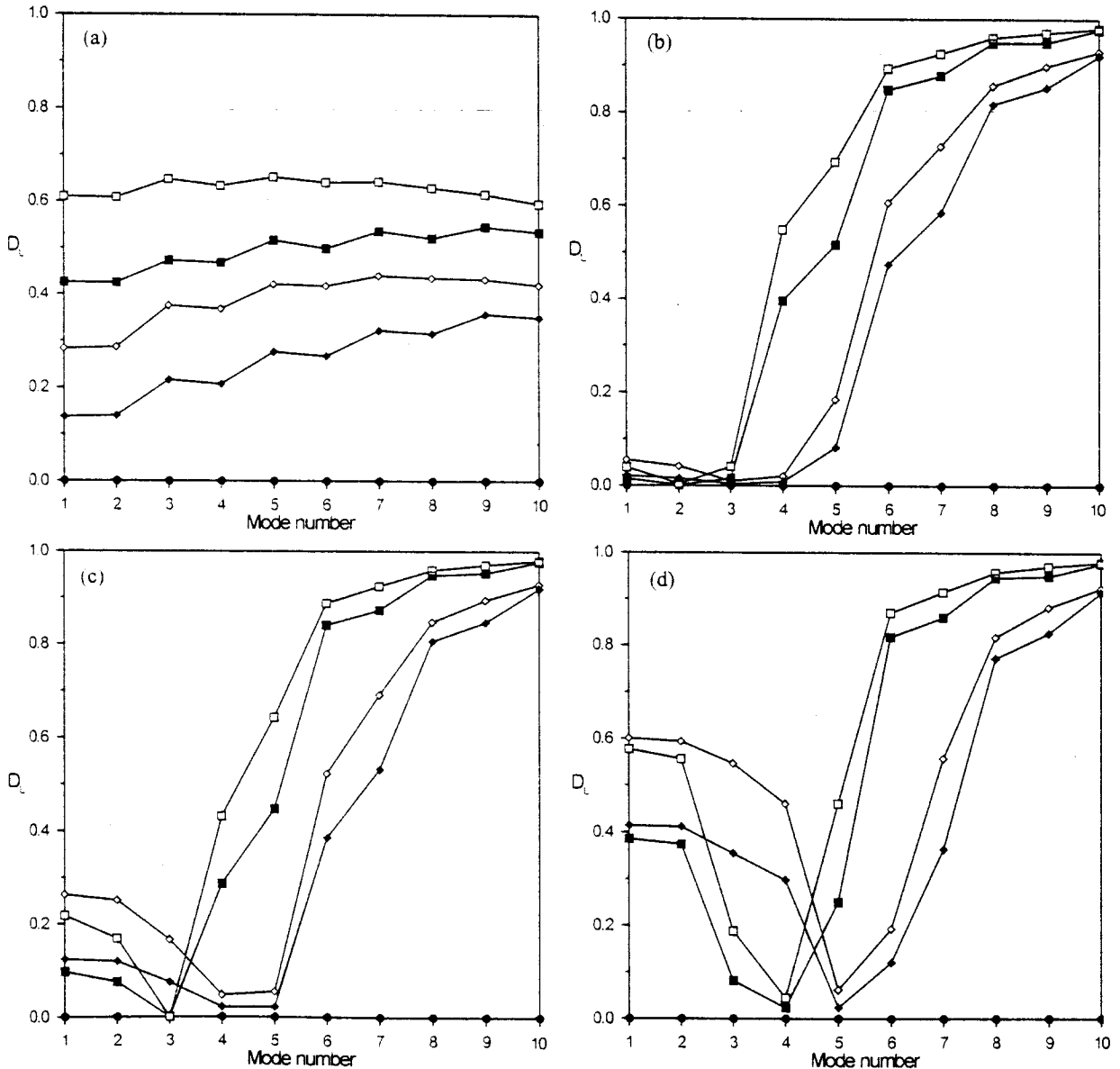


Fig. 6. Influences of the Lumped Rotational Stiffness and the Lumped Rotational Mass of Coupler on Mode Localization. Solid circles (\bullet) on the horizontal axes imply degrees of mode localization of tuned systems. Solid boxes (\blacksquare) and diamonds (\blacklozenge) are of the cases of $\alpha = 0.03$ and hollow boxes (\square) and diamonds (\diamond) are of the cases of $\alpha = 0.05$: (a) $\bar{K} = 3.0, \bar{J} = 0.0$ (diamonds); $\bar{K} = 10.0, \bar{J} = 0.0$ (boxes). (b) $\bar{K} = 0.0, \bar{J} = 0.03$ (diamonds); $\bar{K} = 0.0, \bar{J} = 0.1$ (boxes). (c) $\bar{K} = 3.0, \bar{J} = 0.03$ (diamonds); $\bar{K} = 3.0, \bar{J} = 0.1$ (boxes). (d) $\bar{K} = 10.0, \bar{J} = 0.03$ (diamonds); $\bar{K} = 10.0, \bar{J} = 0.1$ (boxes).

4. Mode Localization of Two Span Beam

In this example study, the influences of a lumped rotational stiffness and a lumped rotational mass constituting a coupler of the simply supported two span beam shown in Fig. 5 on mode localization are studied. The lengths of the spans are assumed as $L_1 = L(1 + \alpha)$ and $L_2 = L(1 - \alpha)$ where L is a reference half-span length and α is disturbance breaking the periodicity of the structure. The cases considered are consistent with those in the previous section and Fig. 4.

In this example study, to facilitate discussion for mode localization of multispan beams, a measure of the degree of mode localization, D_L , is defined as

$$D_L \equiv 2 - \frac{(\bar{y}_1 + \bar{y}_2)^2}{\bar{y}_1^2 + \bar{y}_2^2} \tag{25}$$

where \bar{y}_i is the absolute value of the maximum amplitude associated with the i -th span. The degree of mode localiza-

tion is to be unity, $D_L = 1$, when the mode is extremely localized and is to be zero, $D_L = 0$, when the mode is not localized at all.

Localization curves in Fig. 6(a) show the typical behavior of mode localization and the influences of \bar{K} on mode localization. Degrees of mode localization increase with the increase of α and \bar{K} . The influence of \bar{J} differs from that of \bar{K} and the localization curves in Fig. 6(b) show it. Degrees of mode localization increase with the increases of α , mode number and \bar{J} . That is, the mass of coupler makes the structure sensitive to mode localization and the mass effect is more pronounce in the higher modes. Localization curves plotted in Figs. 6(c) and 6(d) show the combined influences of \bar{K} and \bar{J} . Degree of mode localization decreases with the increase of mode number until certain modes, but after that modes it increases abruptly with mode number. The modes for which mode localization does not occur or is very weak although structural disturbances are severe are referred as delocalized modes. These delocaliza-

Table 1. Dimensionless Eigenvalues, $\lambda L/\pi$, of the System Considered in Fig. 6(a)

Mode Number	$\bar{K} = 3.0, \bar{J} = 0.0$			$\bar{K} = 10.0, \bar{J} = 0.0$		
	$\alpha = 0.01$	$\alpha = 0.03$	$\alpha = 0.05$	$\alpha = 0.01$	$\alpha = 0.03$	$\alpha = 0.05$
1	0.568	0.564	0.558	0.600	0.591	0.581
2	0.625	0.630	0.638	0.625	0.635	0.646
3	1.048	1.038	1.025	1.085	1.068	1.050
4	1.125	1.137	1.153	1.125	1.144	1.165
5	1.537	1.520	1.498	1.574	1.548	1.521
6	1.625	1.645	1.670	1.625	1.654	1.685
7	2.030	2.004	1.974	2.065	2.029	1.994
8	2.125	2.154	2.189	2.125	2.165	2.205
9	2.525	2.490	2.452	2.558	2.512	2.469
10	2.625	2.664	2.708	2.625	2.676	2.726

Table 2. Dimensionless Eigenvalues, $\lambda L/\pi$, of the System Considered in Fig. 6(b)

Mode Number	$\bar{K} = 0.0, \bar{J} = 0.03$			$\bar{K} = 10.0, \bar{J} = 0.0$		
	$\alpha = 0.00$	$\alpha = 0.03$	$\alpha = 0.05$	$\alpha = 0.00$	$\alpha = 0.03$	$\alpha = 0.05$
1	0.491	0.490	0.488	0.470	0.469	0.468
2	0.625	0.627	0.630	0.625	0.625	0.626
3	0.918	0.917	0.916	0.794	0.796	0.798
4	1.125	1.123	1.119	1.125	1.108	1.091
5	1.261	1.267	1.276	1.165	1.184	1.205
6	1.625	1.598	1.572	1.625	1.584	1.554
7	1.671	1.702	1.733	1.638	1.682	1.716
8	2.125	2.073	2.035	2.125	2.066	2.027
9	2.144	2.200	2.246	2.130	2.193	2.239
10	2.625	2.554	2.506	2.625	2.550	2.502

Table 3. Dimensionless Eigenvalues, $\lambda L/\pi$, of the System Considered in Fig. 6(C)

Mode Number	$\bar{K} = 3.0, \bar{J} = 0.03$			$\bar{K} = 3.0, \bar{J} = 0.0$		
	$\alpha = 0.00$	$\alpha = 0.03$	$\alpha = 0.05$	$\alpha = 0.00$	$\alpha = 0.03$	$\alpha = 0.05$
1	0.565	0.561	0.555	0.557	0.553	0.549
2	0.625	0.630	0.637	0.625	0.629	0.635
3	1.002	0.997	0.990	0.876	0.876	0.876
4	1.125	1.129	1.134	1.125	1.111	1.096
5	1.316	1.318	1.322	1.173	1.190	1.209
6	1.625	1.601	1.577	1.625	1.584	1.555
7	1.679	1.706	1.737	1.638	1.682	1.717
8	2.125	2.074	2.035	2.125	2.066	2.027
9	2.145	2.201	2.246	2.131	2.193	2.239
10	2.625	2.554	2.506	2.625	2.550	2.502

Table 4. Dimensionless Eigenvalues, $\lambda L/\pi$, of the System Considered in Fig. 6(D)

Mode Number	$\bar{K} = 10.0, \bar{J} = 0.03$			$\bar{K} = 10.0, \bar{J} = 0.1$		
	$\alpha = 0.00$	$\alpha = 0.03$	$\alpha = 0.05$	$\alpha = 0.00$	$\alpha = 0.03$	$\alpha = 0.05$
1	0.599	0.590	0.581	0.597	0.589	0.580
2	0.625	0.635	0.646	0.625	0.634	0.645
3	1.071	1.058	1.042	1.003	1.000	0.995
4	1.125	1.139	1.157	1.125	1.121	1.116
5	1.440	1.437	1.433	1.206	1.215	1.228
6	1.625	1.613	1.598	1.625	1.585	1.556
7	1.707	1.725	1.751	1.640	1.683	1.717
8	2.125	2.075	2.038	2.125	2.066	2.027
9	2.148	2.202	2.247	2.131	2.193	2.239
10	2.625	2.554	2.506	2.625	2.550	2.502

tion phenomena are more dramatic in cases of the larger stiffness and larger mass. Fig. 6(d). Considering the modes far from the delocalized ones, the behavior of mode localization is governed by \bar{K} for lower modes but by \bar{J} for higher modes. As you can see in Figs. 4 and 5 in the previous section and from Table 1 to 4, a mode in a passband and near the edge of the band is moved to stopband and localized by introducing the span length disturbance α . The delocalized modes are near the points of $C_3 = \pm\pi/2$.

5. Conclusions

In this work, the influences of the stiffness and the mass of the coupler on wave propagation and mode localization have been studied. Some important conclusions drawn in the course of this work can be summarized as follows:

1. The larger stiffness of coupler results in the weaker

internal coupling and the influence of stiffness decreases with the increase of wave frequency.

2. The larger mass of coupler results in the weaker internal coupling and the influence of mass increases abruptly with the increase of wave frequency.
3. The larger stiffness of coupler increases the sensitivity to mode localization of the normal modes of a multispan beam in the lower frequency range.
4. The larger mass of coupler increases the sensitivity to mode localization of the normal modes of a multispan beam in the higher frequency range.
5. Considering the stiffness and the mass of coupler at same time, there is a certain frequency region having relatively wider passband caused by the counter-vailing property between the stiffness and the mass. This leads to delocalization phenomena in some normal modes.

The results of this work may give very useful guide to design a structure insensitive to mode localization.

References

- Anderson, P.W. (1958). "Absence of diffusion in certain random lattices." *Physical Reviews*, Vol. 109, pp. 1492-1505.
- Bendiksen, O.O. (1987). "Mode localization phenomena in large space structures." *American Institute of Aeronautics and Astronautics Journal*, Vol. 25, pp. 1241-1248.
- Bouzit, D. and Pierre, C. (1992). "Vibration confinement phenomena in disordered, mono-coupled, multi-span beams." *Journal of Vibration and Acoustics*, ASME, Vol. 114, No. 4, pp. 521-530.
- Cornwell, P.J. and Bendiksen, O.O. (1987). "Localization of vibration in large space reflectors." *Proceedings of the 28th AIAA/ASME/ASCE/AHS Structures, Structural Dynamics and Materials Conference (Monterey, CA)*, New York, pp. 925-935 (AIAA Paper 87-0949).
- Cornwell, P.J. and Bendiksen, O.O. (1989). "Forced vibrations in large space reflectors with localized modes." *Proceedings of the 30th AIAA/ASME/ASCE/AHS Structures, Structural Dynamics and Materials Conference (Mobile, AL)*, Washington, pp. 188-198 (AIAA Paper 89-1180).
- Cornwell, P.J. and Bendiksen, O.O. (1989). "A numerical study of vibration localization disordered cyclic structures." *Proceedings of the 30th AIAA/ASME/ASCE/AHS Structures, Structural Dynamics and Materials Conference (Mobile, AL)*, Washington, pp. 199-208 (AIAA Paper 89-1181).
- Hodges, C.H. (1982). "Confinement of vibration by structural irregularity." *Journal of Sound and Vibration*, Vol. 82, No. 3, pp. 411-424.
- Kim, D.O. and Lee, I.W. (1998). "Mode localization in simply supported two-span beams of arbitrary span lengths." *Journal of Sound and Vibration*, Vol. 213, No. 5, pp. 952-961.
- Kim, D.O. and Lee, I.W. (1999). "Mode localization in structures consisting of substructures and couplers." *Engineering Structures*, Vol. 22, No. 1, pp. 39-48.
- Langley, R.S. (1995). "Mode localization up to high frequencies in coupled one-dimensional subsystems." *Journal of Sound and Vibration*, Vol. 185, No. 1, pp. 79-91.
- Lust, S.D., Friedmann, P.P. and Bendiksen, O.O. (1993). "Mode localization in multispan beams." *AIAA Journal*, Vol. 31, No. 2, pp. 348-355.
- Pierre, C. and Dowell, E.H. (1987). "Localization of vibrations by the structural irregularity." *Journal of Sound and Vibration*, Vol. 114, No. 3, pp. 549-564.
- Pierre, C., Tang, D.M. and Dowell, E.H. (1987). "Localized vibrations of disordered multi-span beams: theory and experiment." *American Institute of Aeronautics and Astronautics Journal*, Vol. 25, No. 9, pp. 1249-1257.